

Mechanical properties and extended creep behavior of bamboo fiber reinforced recycled poly(lactic acid) composites using the time–temperature superposition principle



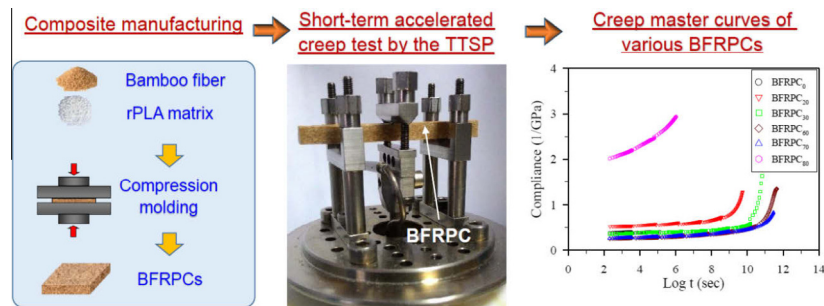
Teng-Chun Yang, Tung-Lin Wu, Ke-Chang Hung, Yong-Long Chen, Jyh-Horng Wu*

Department of Forestry, National Chung Hsing University, Taichung 402, Taiwan

HIGHLIGHTS

- Mechanical and creep properties of BFRPCs with various fiber loadings were studied.
- BFRPC with 60 wt% fiber exhibited the best flexural properties and creep resistance.
- The E' of BFRPCs above the T_g of rPLA increased with increasing fiber loading up to 60 wt%.
- Nearly perfect superposition of master curves was obtained using the TTSP method.
- The modulus of all BFRPCs reduced in the range of 27–40% over a 30-year period.

GRAPHICAL ABSTRACT



ARTICLE INFO

Article history:

Received 10 February 2015
Received in revised form 15 June 2015
Accepted 16 June 2015

Keywords:

Bamboo fiber
Creep behavior
Mechanical property
Poly(lactic acid)
Time–temperature superposition principle

ABSTRACT

The present study investigates mechanical properties and creep resistance of bamboo fiber reinforced recycled PLA composites (BFRPCs). The results revealed that the modulus of rupture and modulus of elasticity of BFRPCs increased with increasing bamboo fiber loading up to 60 wt% and then declined sharply as the fiber increased further. Short-term accelerated creep tests on BFRPCs were conducted at a series of elevated temperatures by time–temperature superposition principle. As a result, the BFRPC with 60 wt% fiber exhibited the best creep resistance among all the BFRPCs, and then decreased when the fiber loading was more than 70 wt%.

© 2015 Elsevier Ltd. All rights reserved.

1. Introduction

In recent years, the depletion of fossil fuels and the growth of environmental awareness have motivated many researchers to develop bio-materials. Consequently, natural fiber biocomposites, such as wood plastic composites (WPCs), have become important

in composite science. WPCs are of great interest in construction applications due to their advantages, including dimensional stability, moisture resistance, mechanical properties, and durability [1–4]. However, one of their disadvantages is the change in WPC mechanical properties with temperature, leading to limits in wider applications. Therefore, it is also important to investigate the temperature sensitivity of WPC properties, such as creep behavior, because WPCs exhibit a strong time–temperature dependent response. On the other hand, it is time-consuming and

* Corresponding author.

E-mail address: eric@nchu.edu.tw (J.-H. Wu).

expensive to conduct full-scale creep tests in a normal time scale. In this study, an accelerated creep test based on the time–temperature superposition principle (TTSP) was implemented to predict the long-term creep response. Methods using this principle have been employed to confirm that TTSP is applicable to various WPCs [5–8].

Among bio-based polymers, poly(lactic acid) (PLA), which is made from renewable raw agricultural materials, is a versatile biodegradable polymer used in many applications. PLA has great potential to replace petroleum-based plastics due to its high stiffness and strength compared with polystyrene. However, the drawbacks of PLA include its brittleness, low thermal resistance, and slow crystallization rate, which limit wider applications. To overcome these drawbacks and reduce fossil fuel consumption, natural fiber reinforced PLA has been studied to improve the characteristics of PLA and obtain fully bio-based composites [9–11]. Compared with inorganic fillers, natural fibers such as wood, bamboo, flax, ramie, jute, kenaf, and hemp have numerous advantages: low cost, low density, high toughness, good specific strength properties, renewability, and biodegradability [9,12–15]. In particular, bamboo fiber reinforcement has great potential to improve the thermal and mechanical properties of PLA composites due to its excellent physical properties [16–19]. Additionally, bamboo fiber is easily obtained because of its wide distribution across Asia [20] and fast growth rate in comparison with other plants having fibers [21–23]. Furthermore, bamboo fiber reinforced PLA composites (BFRPCs) would utilize large amounts of bamboo shavings and sawdust, by-products of the bamboo-processing industry. To date, investigations into BFRPCs focused primarily on the effects of various attributes on the thermal and mechanical properties of the composites, such as fiber type, fiber loading, functional additives, and fiber modification to increase the compatibility between the hydrophilic natural fiber and hydrophobic polymeric matrix [24–26]. However, there is little information available on detailed investigations of dynamic mechanical properties and creep behavior of BFRPCs. Therefore, in addition to qualifying their dynamic mechanical properties and static flexural properties, the main objective of the present study was to investigate the time–temperature dependent response and extended creep behavior of BFRPCs using TTSP.

2. Materials and methods

2.1. Preparation of bamboo fibers and recycled poly(lactic acid)

Dried shavings from 3-year-old kei-chiku bamboo (makino bamboo; *Phyllostachys makinoi* Hayata) were provided by the local bamboo-processing factory. Bamboo fibers were prepared by hammer-milling and sieving and fibers between 30 and 60 mesh were investigated. A recycled PLA (rPLA) was purchased from Orbit Polymers Co., Ltd. (Taichung, Taiwan) and had a melting temperature of 145–155 °C.

2.2. Composite panel manufacture

Manufacturing BFRPCs: the flat platen pressing process was applied in our previous papers [2,27]. The weight ratios of the oven-dried bamboo fibers (moisture content <3%) to rPLA powder were 5/95, 10/90, 20/80, 30/70, 40/60, 50/50, 60/40, 70/30, and 80/20 (wt%). The density of the BFRPCs was $1200 \pm 30 \text{ kg/m}^3$. The dimensions of the BFRPC samples were 300 mm × 200 mm with a thickness of 4 mm. All BFRPCs were produced in a two-step pressing process as follows: (1) hot pressing (2.9 MPa) at 175 °C for 3 min; and (2) finishing by cold pressing until the temperature of BFRPCs decreased to 30 °C.

2.3. Flexural properties

The modulus of rupture (MOR) and modulus of elasticity (MOE) of the samples were determined by a three-point static bending test with a loading speed of 1.7 mm/min and with a span of 64 mm (ASTM D790-07). The dimensions of the sample were 80 mm × 16 mm with a thickness of 4 mm. Five samples of rPLA composites with various fiber loading were tested at 20 °C. The samples were conditioned at 20 °C and 65% relative humidity for a week before testing.

2.4. Dynamic mechanical analysis (DMA) and short-term accelerated creep test

The dynamic mechanical properties of the BFRPCs were measured in single cantilever bending mode (DMA 8000, PerkinElmer) at a heating rate of 2 °C/min and a frequency of 1 Hz. The storage modulus (E') and loss tangent ($\tan \delta$) were recorded in the range of 25–160 °C. The dimensions of the sample were 30 mm × 10 mm with a thickness of 4 mm. Additionally, according to TTSP, a dynamic mechanical analysis (DMA) was carried out to determine the glass transition temperature (T_g) and active energy (E_a). These experiments were conducted in dual cantilever mode under isochronal conditions at frequencies of 4, 8, 12, 16, 20, 24, 28, and 32 Hz. The dimensions of the sample were 50 mm × 10 mm with a thickness of 4 mm. Tests were conducted in the range of 25–120 °C at a scanning rate of 1 °C/min.

TTSP, using a real-time short-term creep response at elevated temperatures, is used to predict the long-term creep performance of the composites. The creep compliance is given by $S(T_{\text{ref}}, t) = S(T_{\text{elev}}, t/\alpha_T)$, where S is the creep compliance as a function of temperature and time, T_{ref} is the reference temperature, T_{elev} is the elevated temperature, and α_T is the shift factor. The master curve of creep compliance and the activation energy of the glass transition relaxation were also determined by DMA. Creep and creep recovery cycles were conducted at isotherms between 20 and 50 °C in intervals of 5 °C. A three-point bending mode with a span of 40 mm was used. For each isotherm, 30% of the average flexural strength was applied for 1 h, followed by a 1 h recovery period.

2.5. Static analysis

All results are expressed as the mean ± SD. The statistical analysis was performed with one-way ANOVA and Scheffe's post hoc test. The results with $P < 0.05$ were considered to be statistically significant.

3. Results and discussion

3.1. Density, moisture content, and static flexural properties of the samples

The density, moisture content, and flexural properties of the BFRPCs are summarized in Table 1. In general, density and moisture content may directly affect the flexural properties of a polymer composite. Except for the density of BFRPC₈₀ ($\sim 999 \text{ kg/m}^3$), there was no statistical significance ($P > 0.05$) in density among all composites ($\sim 1200 \text{ kg/m}^3$). The decrease in the density of BFRPC₈₀ is attributed to the observable thickness swelling that occurred after compression molding. It can be seen that moisture content increased with increasing fiber loading. With the addition of 80 wt% fiber to PLA, the moisture content increased significantly from 0.4% (BFRPC₀) to 3.9% ($P < 0.05$). As expected, the addition of more fiber to a matrix leads to higher moisture content because

Table 1
Density, moisture content, and flexural properties of various BFRPCs.

Code	Bamboo fiber (wt%)	Density (kg/m ³)	Moisture content (%)	Flexural properties	
				MOR (MPa)	MOE (GPa)
BFRPC ₀	0	1216 ± 41 ^a	0.4 ± 0.0 ^f	22.3 ± 0.4 ^{cd}	3.22 ± 0.09 ^b
BFRPC ₅	5	1179 ± 19 ^a	0.7 ± 0.1 ^{ef}	14.1 ± 1.9 ^d	3.27 ± 0.20 ^b
BFRPC ₁₀	10	1193 ± 36 ^a	0.9 ± 0.2 ^{edf}	14.6 ± 1.0 ^d	3.42 ± 0.24 ^b
BFRPC ₂₀	20	1133 ± 46 ^a	1.3 ± 0.1 ^{ed}	17.2 ± 2.7 ^d	3.34 ± 0.46 ^b
BFRPC ₃₀	30	1176 ± 32 ^a	1.4 ± 0.1 ^d	29.1 ± 1.1 ^c	3.87 ± 0.83 ^b
BFRPC ₄₀	40	1195 ± 12 ^a	2.3 ± 0.3 ^c	38.8 ± 2.2 ^b	5.80 ± 0.34 ^a
BFRPC ₅₀	50	1247 ± 15 ^a	2.7 ± 0.2 ^c	46.5 ± 1.2 ^b	6.87 ± 0.21 ^a
BFRPC ₆₀	60	1228 ± 12 ^a	2.9 ± 0.2 ^{bc}	56.1 ± 2.6 ^a	7.28 ± 0.17 ^a
BFRPC ₇₀	70	1155 ± 19 ^a	3.5 ± 0.3 ^{ab}	47.9 ± 5.1 ^{ab}	6.26 ± 0.41 ^a
BFRPC ₈₀	80	0999 ± 32 ^b	3.9 ± 0.2 ^a	21.8 ± 2.4 ^{cd}	3.18 ± 0.59 ^b

Values are means ± SD ($n = 5$). Different letters within a column indicate significant difference at $P < 0.05$.

the hydrophilic fiber easily absorbs water from the atmosphere. The water in composites can be stored in the fiber cell walls, the cell lumens, and/or the voids between the lignocellulose and the polymer matrix [28,29]. As shown in Table 1, the moisture content of all the BFRPCs is far below fiber saturation point. Accordingly, in the present study, it seems that the water was located primarily in the cell walls of the bamboo fibers.

On the other hand, Table 1 shows that both the modulus of rupture (MOR) and modulus of elasticity (MOE) of BFRPCs increased with increasing fiber loading up to 60 wt%, at which point a drastic decrease in the flexural properties was observed when the fiber loading was more than 60 wt%. Thus, the BFRPC with 60 wt% fiber exhibited the best flexural properties, with MOR and MOE values of 56.1 MPa and 7.28 GPa, respectively. Stiffer bamboo fiber plays a role in stress transition in a composite, leading to improvement of the flexural properties. However, when the fiber loading reached 80 wt%, the MOR and MOE decreased to 21.8 MPa and 3.18 GPa, respectively. The mechanical properties of the composites are negatively affected by various factors, including poor fiber dispersion caused by intermolecular hydrogen bonding and the wide polarity differences of the surfaces that retard the polymer/fiber bonding interaction [30]. The decline in flexural properties may be attributable to the aggregation of the woody materials. Poor interfacial adhesion leads to composites with poor mechanical properties [27,31–33]. Reports by Lee et al. [2,34] demonstrated that the MOR and MOE of various WPCs were in the range of 8.5–25.3 MPa and 1.0–2.4 GPa, respectively; even the flexural properties of BFRPC with 80 wt% bamboo fiber were higher than those of conventional WPCs.

3.2. Dynamic mechanical properties

Hong et al. [35] noted that dynamic mechanical flexural properties exhibit sensitivity to the interfacial adhesion between the lignocellulose and the polymer matrix. Fig. 1 shows the plots of the storage modulus (E') and loss tangent ($\tan \delta$) as a function of fiber loading level. As illustrated in Fig. 1a, a noticeable drop in E' of all the composites was observed near the T_g (ca. 50 °C) of the PLA due to the increase in chain mobility of the PLA matrix [36]. For BFRPC₀ (neat rPLA), the E' dropped dramatically to 1.73×10^{-3} GPa at 98 °C and then increased to 3.83×10^{-2} GPa at 120 °C. The latter increase in E' can be attributed to the annealing crystallization of the rPLA matrix. A similar result was also reported by Suryanegara et al. [37]. However, when bamboo fibers were added into the rPLA matrix, the E' of BFRPCs increased with increasing fiber loading up to 60 wt% at temperatures above T_g . Among all the BFRPCs, it can be seen that BFRPC₆₀ exhibited the highest thermal resistance: the E' increased dramatically from

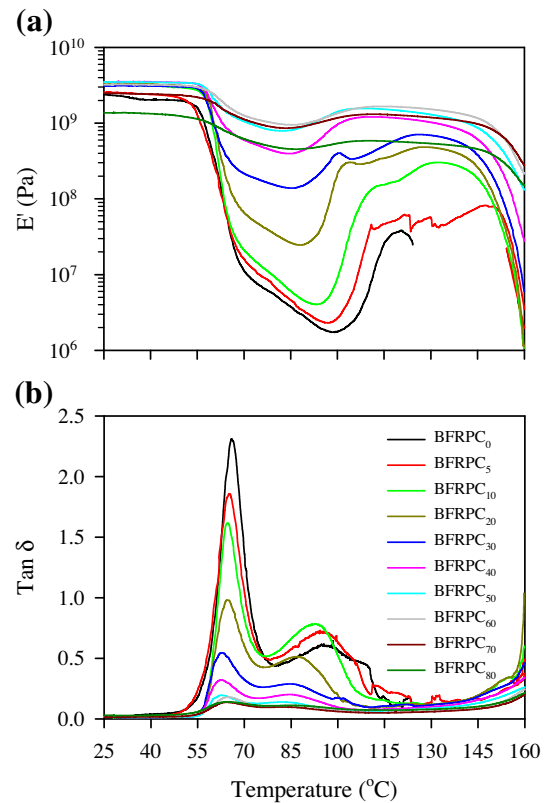


Fig. 1. Effect of bamboo fiber loading level on the storage modulus (a) and $\tan \delta$ (b) of BFRPCs.

the original 1.73×10^{-3} to 1.27 GPa at 98 °C. This result indicated that the addition of the appropriate bamboo fiber can significantly improve the thermal resistance of rPLA composites.

$\tan \delta$, a measure of material-related damping properties, is an indication of molecular motion in materials, which contributes at the interface to damping or energy dissipation [30,35]. As shown in Fig. 1b, two remarkable peaks were observed at approximately 65 and 98 °C. The former peak is the T_g of amorphous rPLA and the latter peak is the T_g of partially crystalline rPLA which is induced by annealing at elevated temperatures during the process. Both peaks decreased with increased fiber loading. In particular, when 80 wt% fiber was added into rPLA matrix, the $\tan \delta$ intensity at 65 °C declined by 94%, from the original 2.18 to 0.14.

3.3. Extended creep behavior of BFRPCs using TTSP

This section will outline the use of TTSP to predict the long-term creep behavior of the composites from short-term accelerated creep tests at a range of elevated temperatures. DMA is appropriate for this test because it is capable of testing at a wide range of temperatures. Using BFRPC₆₀ as an example, Fig. 2a shows the creep compliance with elevated temperature in the actual time for the entire duration, and Fig. 2b shows the unshifted and shifted short-term creep compliance curves of BFRPC₆₀ at all the temperatures tested plotted against the test time in a log scale. According to the reduced time using a shift factor (α_T) calculated from TTSP, the creep curves at elevated temperatures were shifted along the time axis to the right.

Regarding the shift factor, there are two methods that are being used for WPCs: the William–Landel–Ferry (WLF) equation and the Arrhenius equation. For the WLF equation, the material is tested at working temperatures in the range from T_g to $T_g + 100$ °C [38].

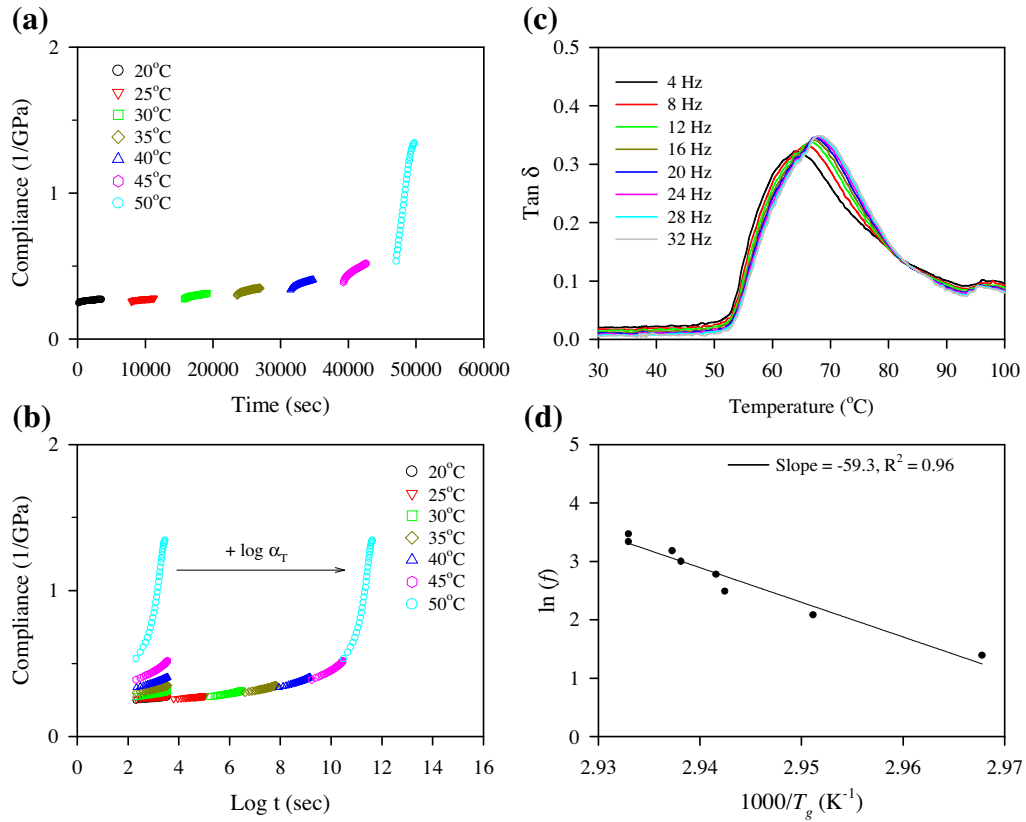


Fig. 2. The creep compliance of BFRPC₆₀ at elevated temperatures in the actual test (a). Unshifted and shifted creep compliance of BFRPC₆₀ using a reference temperature of 20 °C against the test time in a log scale (b). Tan δ curves for a range of frequencies at a heating rate of 1 °C/min (c). Frequency in a log scale versus the inverse of T_g (d).

However, PLA is not appropriate for this method because it exhibits a rubbery state or melting state in this working temperature range (60–160 °C). Therefore, the Arrhenius equation was used for BFRPC in this study. The shift factor, $\log \alpha_T$, can be related to temperature and activation energy using the following equation:

$$\log \alpha_T = \frac{E_a}{R} \left(\frac{1}{T} - \frac{1}{T_{ref}} \right) \times \log e$$

where α_T is the horizontal shift factor, E_a is the activation energy of the glass transition relaxation (kJ/mol), T_{ref} is the reference temperature (K), T is the test temperature (K), and R is the universal gas constant (8.314 J/K/mol) [5,39]. E_a was estimated from the frequency dependence of the T_g of BFRPC measured from DMA and must be overcome for the occurrence of molecular motion causing the transition [40].

Fig. 2c shows $\tan \delta$ curves for a range of frequencies at a heating rate of 1 °C/min. The T_g at different frequencies was determined from the peak of the $\tan \delta$ curves and the E_a is calculated from the slope of the plot of $\ln(f)$ versus $1/T_g$ using the following equation:

$$E_a = -R \frac{d(\ln(f))}{d(1/T_g)}$$

where f is frequency (Hz) and T_g is the glass transition temperature. As shown in Fig. 2d, frequency on a log scale versus the inverse of T_g was plotted.

A linear regression was performed on the slope and E_a was calculated. According to this calculation, the effect of bamboo fiber loading level on the E_a of BFRPCs is shown in Table 2. The result indicated that the E_a values of BFRPCs with various amount of bamboo fiber were in the range of 428.5–493.2 kJ/mol. Consequently, the creep compliance master curves of the various BFRPCs

generated using shift factors are estimated from a constant activation energy assumption. The master curves were modeled with the Findley power law [41], which is presented in following equation: $S(t) = S_0 + at^b$, where $S(t)$ is the time-dependent compliance, S_0 is the instantaneous elastic compliance, a and b are constant numbers, and t is the elapsed time. The creep curves of the various BFRPCs in a log time scale are shown in Fig. 3a, and the result revealed that the compliance decreased with increasing fiber loading up to 60 wt%. Among all the BFRPCs, the compliance of BFRPC₆₀ was the lowest during the creep duration. When 80 wt% fiber was added in the rPLA matrix, however, the compliance increased dramatically. Fig. 3b shows the creep master curves in a normal time scale; the instantaneous elastic compliances (S_0) and the predicted reductions in the modulus levels of all the BFRPCs over 1–30 year periods are tabulated in Table 2. The S_0 of BFRPC₆₀ was the lowest (0.23 GPa⁻¹) among all the BFRPCs. For the predicted compliance, BFRPC₃₀ showed 0.42, 0.44, 0.46, and 0.47 GPa⁻¹ at 1, 5, 15, and 30 years, respectively. Once the fiber loading increased to 60 wt%, the predicted compliance declined to 0.33, 0.36, 0.37, and 0.39 GPa⁻¹ at 1, 5, 15, and 30 years, respectively. These results implied that the increase in bamboo fiber loading significantly improved the creep resistance of BFRPCs due to the better stiffness and heat conduction of the bamboo fiber. These findings are similar to the flexural properties data. However, when the fiber loading reached 80 wt%, like BFRPC₀, the predicted compliance of BFRPC₈₀ was not detectable because the composite was fractured at less than 1-year period. Furthermore, in order to estimate the creep resistance of a sample under long-term conditions, the reduction in modulus was calculated by the following equation: modulus reduction (%) = $[1 - S_0/S(t)] \times 100$ [6]. As shown in Table 2, the modulus of all BFRPCs reduced in the range of 27–40% over a 30-year period. However, according to the increase

Table 2
Activation energy and the predicted reduction in modulus of various BFRPCs using a reference temperature of 20 °C.

Code	S_0 (GPa ⁻¹)	a	b	$S(t)$ (GPa ⁻¹)				Reduction in modulus (%)				Activation energy (kJ/mol)	
				Time (Years)				Time (Years)					
				1	5	15	30	1	5	15	30		
BFRPC ₀	ND	ND	ND	ND	ND	ND	ND	ND	ND	ND	ND	ND	428.5
BFRPC ₂₀	0.54	3.47×10^{-4}	0.32	0.63	0.69	0.75	0.80	13.8	21.2	27.7	32.4	440.9	
BFRPC ₃₀	0.34	7.21×10^{-3}	0.14	0.42	0.44	0.46	0.47	19.2	22.7	25.4	27.1	473.4	
BFRPC ₆₀	0.23	9.68×10^{-3}	0.13	0.33	0.36	0.37	0.39	29.4	34.2	37.5	39.7	493.2	
BFRPC ₇₀	0.25	7.83×10^{-3}	0.14	0.34	0.36	0.37	0.39	25.7	30.6	34.1	36.4	477.9	
BFRPC ₈₀	1.77	1.01×10^{-1}	0.18	ND	ND	ND	ND	ND	ND	ND	ND	ND	448.3

$S(t) = S_0 + at^b$, where $S(t)$ is the time-dependent compliance, S_0 is the instantaneous elastic compliance, a and b are constant numbers. ND: not detectable.

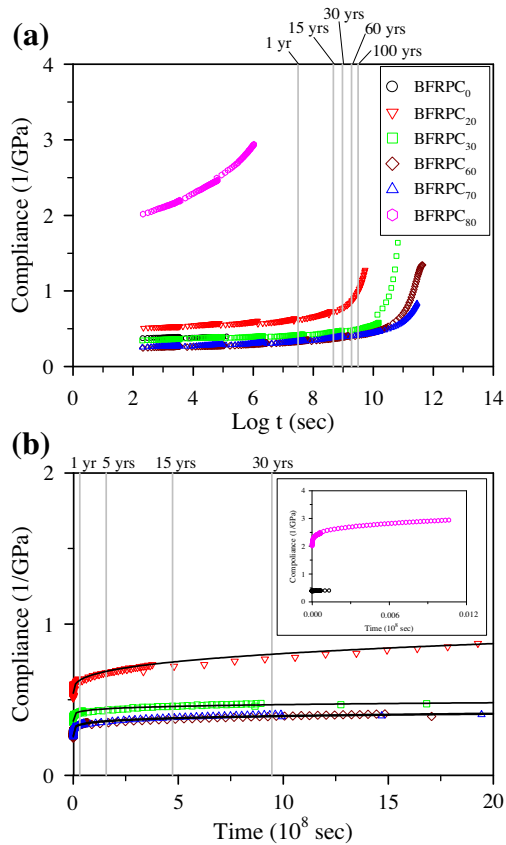


Fig. 3. Creep master curves of various BFRPCs in a log time scale (a) and in a normal time scale (b) using a reference temperature of 20 °C.

rate of the compliance (b value of the Findley power law), the BFRPC₆₀ showed the smallest b value (0.13) among all the BFRPCs. Taken together, the results indicated that the 60 wt% fiber-loaded BFRPC exhibited the best creep resistance.

4. Conclusions

Bamboo fibers exhibit excellent reinforcing effects on the thermal resistance, flexural properties, and creep resistance of recycled poly(lactic acid) (rPLA) composites. Although moisture content increased with increasing bamboo fiber loading, the modulus of rupture (MOR) and modulus of elasticity (MOE) of bamboo fiber reinforced rPLA composites (BFRPCs) were enhanced with increasing fiber loading up to 60 wt%. Stiffer bamboo fiber plays a role in stress transition to improve the flexural properties of a composite. Regarding viscoelastic properties, the storage modulus (E') of all the BFRPCs decreased at temperatures above T_g , but E' increased

with increasing fiber loading up to 60 wt%. In addition, the BFRPC with 60 wt% fiber exhibited the best creep resistance among all the BFRPCs according to instantaneous elastic compliance and the increase rate of the compliance of the Findley power law. These results indicate that the addition of bamboo fiber to BFRPCs significantly improved creep resistance due to the better stiffness and heat conduction of bamboo fiber. Accordingly, the addition of bamboo fibers into an rPLA matrix can improve its thermal resistance, flexural properties, and creep resistance, especially with 60 wt% fiber.

Acknowledgement

This work was financially supported by a research Grant from the Ministry of Science and Technology, Taiwan (MOST 102-2628-B-005-006-MY3).

References

- [1] A. Klyosov, *Wood-Plastic Composites*, John Wiley & Sons, New Jersey, 2007.
- [2] C.-H. Lee, T.-L. Wu, Y.-L. Chen, J.-H. Wu, Characteristics and discrimination of five types of wood-plastic composites by Fourier transform infrared spectroscopy combined with principal component analysis, *Holzforchung* 64 (2010) 699–704.
- [3] V. Kumar, L. Tyagi, S. Sinha, Wood flour – reinforced plastic composites: a review, *Rev. Chem. Eng.* 27 (2011) 253–264.
- [4] R.R. Devi, M. Mandal, T.K. Maji, Physical properties of simul (red-silk cotton) wood (*Bombax ceiba* L.) chemically modified with styrene acrylonitrile co-polymer and nanoclay, *Holzforchung* 66 (2012) 365–371.
- [5] A.J. Nuñez, N.E. Marcovich, M.I. Aranguren, Analysis of the creep behavior of polypropylene-woodflour composites, *Polym. Eng. Sci.* 44 (2004) 1594–1603.
- [6] W.K. Goertzen, M.R. Kessler, Creep behavior of carbon fiber/epoxy matrix composites, *Mater. Sci. Eng. A – Struct. Mater. Prop. Microstruct. Process* 421 (2006) 217–225.
- [7] J. Chen, D.J. Gardner, Dynamic mechanical properties of extruded nylon-wood composites, *Polym. Compos.* 29 (2008) 372–379.
- [8] P. Dasappa, P. Lee-Sullivan, X. Xiao, Temperature effects on creep behavior of continuous fiber GMT composites, *Compos. Part A – Appl. Sci.* 40 (2009) 1071–1081.
- [9] K. Oksman, M. Skrifvars, J.-F. Selin, Natural fibres as reinforcement in polylactic acid (PLA) composites, *Compos. Sci. Technol.* 63 (2003) 1317–1324.
- [10] M.S. Huda, L.T. Drzal, A.K. Mohanty, M. Misra, Chopped glass and recycled newspaper as reinforcement fibers in injection molded poly(lactic acid) (PLA) composites: a comparative study, *Compos. Sci. Technol.* 6 (2006) 1813–1824.
- [11] T. Mukherjee, N. Kao, PLA based biopolymer reinforced with natural fibre: a review, *J. Polym. Environ.* 19 (2011) 714–725.
- [12] B. Xu, J. Simonsen, W.E. Rochefort, Creep resistance of wood-filled polystyrene/high-density polyethylene blends, *J. Appl. Polym. Sci.* 79 (2001) 418–425.
- [13] F. Zhang, T. Endo, W. Qiu, L. Yang, T. Hirotsu, Preparation and mechanical properties of composite of fibrous cellulose and maleated polyethylene, *J. Appl. Polym. Sci.* 84 (2002) 1971–1980.
- [14] M.A.S.A. Samir, F. Alloin, A. Dufresne, Review of recent research into cellulosic whiskers, their properties and their application in nanocomposite field, *Biomacromolecules* 6 (2005) 612–626.
- [15] N. Saba, M.T. Paridah, M. Jawaid, Mechanical properties of kenaf fibre reinforced polymer composite: a review, *Constr. Build. Mater.* 76 (2015) 87–96.
- [16] G. Yang, Y. Zhang, H. Shao, X. Hu, A comparative study of bamboo Lyocell fiber and other regenerated cellulose fibers, *Holzforchung* 63 (2009) 18–22.
- [17] Y. Yu, G. Tian, H. Wang, B. Fei, G. Wang, Mechanical characterization of single bamboo fibers with nanoindentation and microtensile technique, *Holzforchung* 65 (2011) 113–119.

- [18] C. Qu, T. Kishimoto, S. Ogita, M. Hamada, N. Nakajima, Dissolution and acetylation of ball-milled birch (*Betula platyphylla*) and bamboo (*Phyllostachys nigra*) in the ionic liquid [Bmim]Cl for HSQC NMR analysis, *Holzforschung* 66 (2012) 607–614.
- [19] J. Gottron, K.A. Harries, Q. Xu, Creep behaviour of bamboo, *Constr. Build. Mater.* 66 (2014) 79–88.
- [20] J.M.O. Scurlock, D.C. Dayton, B. Hames, Bamboo: an overlooked biomass resource?, *Biomass Bioenergy* 19 (2000) 229–244; J.M.O. Scurlock, D.C. Dayton, B. Hames, Bamboo: an overlooked biomass resource?, *Holzforschung* 58 (2000) 537–543.
- [21] Y. Mi, X. Chen, Q. Guo, Bamboo fiber-reinforced polypropylene composites: crystallization and interfacial morphology, *J. Appl. Polym. Sci.* 64 (1997) 1267–1273.
- [22] T. Fujii, K. Okubo, The effective utilization of bamboo as a sustainable reproducible natural resources, *Seikeikako* 15 (2003) 605–611.
- [23] S.-H. Lee, T. Ohkita, Bamboo fiber (BF)-filled poly(butylene succinate) biocomposite – effect of BF-e-MA on the properties and crystallization kinetics, *Holzforschung* 58 (2004) 537–543.
- [24] S.-H. Lee, T. Ohkita, K. Kitagawa, Eco-composite from poly(lactic acid) and bamboo fiber, *Holzforschung* 58 (2004) 529–536.
- [25] S.-H. Lee, S. Wang, Biodegradable polymers/bamboo fiber biocomposite with bio-based coupling agent, *Compos. Part A – Appl. Sci.* 37 (2006) 80–91.
- [26] R. Tokoro, D.M. Vu, K. Okubo, T. Tanaka, T. Fujii, T. Fujiura, How to improve mechanical properties of polylactic acid with bamboo fibers, *J. Mater. Sci.* 43 (2008) 775–787.
- [27] K.-C. Hung, J.-H. Wu, Mechanical and interfacial properties of plastic composite panels made from esterified bamboo particles, *J. Wood Sci.* 56 (2010) 216–221.
- [28] S. Das, A.K. Sara, P.K. Choudhury, B.C. Mitra, T. Todd, S. Lang, Effect of steam pretreatment of jute fiber on dimensional stability of jute composite, *J. Appl. Polym. Sci.* 76 (2000) 1652–1661.
- [29] T.-L. Wu, Y.-C. Chien, T.-Y. Chen, J.-H. Wu, The influence of hot-press temperature and cooling rate on thermal and physicochemical properties of bamboo particle-poly(lactic acid) composites, *Holzforschung* 67 (2013) 325–331.
- [30] Y.-L. Chen, C.-Y. Lin, T.-L. Wu, M.-J. Chung, T.-Y. Chen, T.-H. Yang, et al., Evaluation and application of the invasive weed *Mikania micrantha* as an alternative reinforcement in recycled high density polyethylene, *Bioresources* 7 (2012) 2403–2417.
- [31] S.K. Najafi, E. Hamidinia, M. Tajvidi, Mechanical properties of composites from sawdust and recycled plastics, *J. Appl. Polym. Sci.* 100 (2006) 3641–3645.
- [32] R. Bouza, A. Lasagabaster, M.J. Abad, L. Barral, Effect of vinyltrimethoxy silane on thermal properties and dynamic mechanical properties of polypropylene-wood flour composites, *J. Appl. Polym. Sci.* 109 (2008) 1197–1204.
- [33] S.H. Mansour, J.N. Asaad, B.A. Iskander, S.Y. Tawfik, Influence of some additives on the performance of wood flour/polyolefin composites, *J. Appl. Polym. Sci.* 109 (2008) 2243–2249.
- [34] C.-H. Lee, K.-C. Hung, Y.-L. Chen, T.-L. Wu, J.-H. Wu, Effects of polymeric matrix on accelerated UV weathering properties of wood-plastic composites, *Holzforschung* 66 (2012) 981–987.
- [35] C.K. Hong, N. Kim, S.L. Kang, C. Nah, Y.S. Lee, B.H. Cho, et al., Mechanical properties of maleic anhydride treated jute fibre/polypropylene composites, *Plast. Rubber Compos.* 37 (2008) 325–330.
- [36] B.-H. Lee, H.-S. Kim, S.-H. Lee, J. Kim, J.-R. Dorgan, Bio-composites of kenaf fibers in polylactide: role of improved interfacial adhesion in the carding process, *Compos. Sci. Technol.* 69 (2009) 2573–2579.
- [37] L. Suryanegara, A.N. Nakagatio, H. Yano, The effect of crystallization of PLA on the thermal and mechanical properties of microfibrillated cellulose-reinforced PLA composites, *Compos. Sci. Technol.* 69 (2009) 1187–1192.
- [38] J.D. Ferry, *Viscoelastic Properties of Polymers*, John Wiley & Sons, New York, 1980.
- [39] Y. Xu, Q. Wu, Y. Lei, F. Yao, Creep behavior of bagasse fiber reinforced polymer composites, *Bioresour. Technol.* 101 (2010) 3280–3286.
- [40] G. LaPlante, P. Lee-Sullivan, Moisture effects on FM300 structural film adhesive: stress relaxation, fracture toughness, and dynamic mechanical analysis, *J. Appl. Polym. Sci.* 95 (2005) 1285–1294.
- [41] W.N. Findley, J.S. Lai, K. Onaran, *Creep and Relaxation of Nonlinear Viscoelastic Materials – with an Introduction to Linear Viscoelasticity*, Dover Publications, New York, 1976.